

Light scattering under conditions of nonstationary electromagnetically induced transparency

N.V. Larionov, I.M. Sokolov

Abstract. The propagation of probe radiation pulses in ultracold atomic ensembles is studied theoretically under conditions of electromagnetically induced transparency. The pulse ‘stopping’ process is considered which takes place upon nonadiabatic switching off and subsequent switching on the control field. We analysed the formation of an inverted recovered probe radiation pulse, i.e. the pulse propagating in the direction opposite to the propagation direction before the pulse stopping. Based on this analysis, a scheme is proposed for lidar probing atomic or molecular clouds in which the probe pulse penetrates into a cloud over the specified depth, while information on the cloud state is obtained from the parameters of the inverted pulse. Calculations are performed for an ensemble of ^{87}Rb atoms.

Keywords: electromagnetically induced transparency, light scattering, radiation transfer, ‘stopping of light’, lidar probing, atomic traps.

1. Introduction

The creation of systems with the specified optical properties and the search for methods for rapid controlling these properties is one of the most important problems of modern quantum optics and quantum electronics. The possibility of changing the optical properties of matter by exposing it to the additional, so-called control coherent radiation attracts great recent interest. Such an exposure produces laser-induced coherence in atomic and molecular systems or solids, resulting in a substantial modification of their optical characteristics. This modification can be observed experimentally by the properties of a weak probe radiation. The laser-induced atomic coherence forms the basis of well-studied optical phenomena such as coherent population trapping and electromagnetically induced transparency (EIT) as well as of some comparatively new phenomena called the slowing of light and stopping of light (see reviews [1–3] and references therein).

Along with analysis of the physical properties of induced phenomena, their possible applications in quantum magnetometry, frequency standards, lasers, telecommunication and optical calculation devices, and in the development of new methods for optical information storage (in particular, quantum information) are widely discussed. In this paper, we propose and analyse theoretically the possible application of EIT for optical probing of atomic ensembles.

At present optical methods for diagnostics of atomic and molecular systems are widely used. The information on the state of the medium under study is obtained from the intensity, polarisation, and spectra of transmitted or scattered radiation. However, all these methods have an important disadvantage because the properties of radiation detected in experiments are determined by its evolution along the entire propagation path in the medium. Thus, these methods give only the integral information, which complicates the interpretation and determination of the local properties of systems under study, especially in the case of a large optical thickness and a considerable spatial inhomogeneity.

The method that we propose here is based on the analysis of the attenuation of a probe pulse, which is caused by incoherent scattering and occurs even under EIT conditions [4–7]. The type of attenuation depends not only on the probe-pulse parameters, for example, its spectral width, but also on the properties of the medium such as the concentration of atoms, their velocity, the presence of impurities for which EIT conditions are not fulfilled, the type of interatomic interaction, etc. The method also assumes the use of the effect of stopping light. It is known that the switching on a control field can ‘stop’ a probe pulse at an arbitrary depth in a medium. In this case, the probe pulse disappears and the information on its properties is preserved in the form of a low-frequency atomic coherence. To read this information, i.e. to reconstruct the pulse, it is necessary to switch on the control field again. It is important that the parameters of the reconstructed pulse substantially depend on the properties of the control field upon reading. In particular, it is possible to reconstruct the inverted pulse propagating oppositely to the initial pulse. This occurs if the direction of the wave vector of the control field during reading is opposite to its direction during recording [8–10]. Thus, stopping the probe pulse followed by the change of its propagation direction to the opposite one allows the lidar probing of the system under study by a specified depth. In this case, as in traditional detection methods, the difference of the detected pulse from the initial one is determined by its attenuation over its propagation path. However, first, this

N.V. Larionov, I.M. Sokolov St. Petersburg State Polytechnic University, ul. Politekhnicheskaya 29, 195251 St. Petersburg, Russia; e-mail: larionov-x@rambler.ru, IMS@quark.stu.neva.ru

Received 5 July 2007

Kvantovaya Elektronika 37 (12) 1130–1136 (2007)

Translated by M.N. Sapozhnikov

path passes only through a part of the atomic or molecular ensemble and, second, a comparison of two pulses stopped in different but close regions allows one to make certain conclusions on the local properties of this ensemble.

In this paper, we consider the stopping of light and the formation of inverted pulses in atomic clouds cooled in traps. On the one hand, this choice is determined by their possible practical applications, and on the other – by the lack of reliable detailed information on their shape, the spatial density distribution, and the atomic velocity.

In section 2, we consider the general theory of radiation transfer under the conditions of nonstationary EIT by using the Keldysh diagrammatic technique. We obtained the analytic expressions for the dielectric susceptibility tensor of an inhomogeneous ensemble for the case of the instant switching on and off the control field taking into account the real Zeeman and hyperfine structures of atomic levels. The transformation of a Gaussian probe pulse during its propagation, recording, and reading is analysed in section 3 by solving numerically the radiation transfer equation. In this section, the intermediate processes caused by non-adiabatic switching off the control field are also studied and the basic results of the paper are formulated.

2. Application of the diagrammatic technique to describe radiation transfer under nonstationary EIT conditions

We will analyse the efficiency of our method by the example of an ensemble of ^{87}Rb atoms cooled in a magneto-optical trap. Figure 1 shows the scheme of the experiment on observation of an inverted probe radiation pulse and the structure of operating atomic transitions.

The control field with the wave vector \mathbf{k}_c directed along the positive direction of the z axis is switched off when the probe pulse propagating in the same direction has entered the atomic medium completely or partially. The control field is switched on again after some time, however its wave vector \mathbf{k}'_c is now oriented in the opposite direction. The reconstructed probe pulse is detected with a photodetector PD after reflection from a beamsplitter BS. Probe radiation is filtered with a spectral filter (analyser) SF.

The operating transitions for the control and probe fields are chosen by assuming that only atoms at the hyperfine-structure level $F=1$ of the ground state are confined in a trap upon cooling. It is assumed that the probe field is quasi-resonant with the $F=1 \rightarrow F'=1$ transition (D_1 line) and the control field is quasi-resonant with the $F=2 \rightarrow F'=1$ transition. The distribution of atoms among Zeeman sublevels of the $F=1$ state is assumed uniform due to virtually isotropic irradiation upon laser cooling. The excited-state hyperfine splitting is 816.7 MHz, which exceeds the excited-level width more than by two orders of magnitude. Therefore, the $F'=2$ sublevel is neglected in calculations. We also consider only the case of collinear geometry, when the wave vectors of the probe and control fields during excitation of the coherent state (polariton recording) are directed along the same axis, which we choose as the quantisation axis. Polarisation of the control and probe fields are assumed circular for definiteness, the control field being right-hand polarised and the probe field being either right-hand or left-hand circularly polarised (Fig. 1 corresponds to the latter case).

Atomic clouds in magneto-optical traps have character-

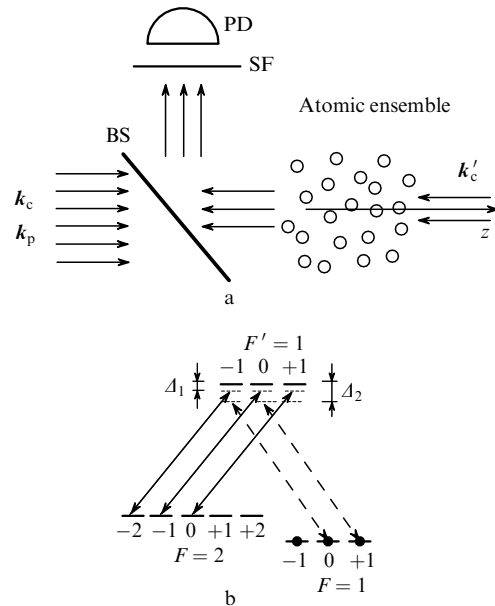


Figure 1. Schemes of the experiment (a) and operating transitions (b): PD: photodetector; SF: spectral filter; BS: beamsplitter; \mathbf{k}_p is the wave vector of the probe field; \mathbf{k}_c and \mathbf{k}'_c are the wave vectors of the control field at different experimental stages.

istic temperatures between 50 and 100 μK . In this case, Doppler shifts are considerably smaller than the widths of excited-state levels. For typical control-field intensities used in light stopping experiments, Doppler shifts are also considerably smaller than the spectral widths of induced transparency bands related to EIT. For this reason, we will assume that atoms are at rest. Note that the assumptions about the collinearity of the fields and immobility of atoms are not necessary. The collinearity is important in light stopping experiments because it allows one to increase considerably the ‘stopping time’ by decreasing the destruction rate of low-frequency coherence caused by atomic motion [11]. If probing is performed by using EIT, the time during which the control field is switched off can be made arbitrarily small, and the atomic motion can be considered in the general calculation scheme.

We will describe the propagation of light in an atomic cloud under nonstationary EIT conditions by using the Green function formalism. The application of this formalism to describe radiation transfer in atomic clouds cooled in a magneto-optical trap is described in detail in recent review [12]. An example when the evolution of the atomic subsystem is determined by the control field, along with other factors, was considered in [7]. The approach developed in [7, 12] can be generalised to the case considered here. This generalisation can be performed by several methods. We will use here the Konstantinov–Perel–Keldysh diagrammatic technique [13–16] for nonequilibrium systems, which was earlier used successfully for solving the problems of scattering of light by ultracold clouds [17].

The source of information on the state of a medium in the probe method considered in our paper is the properties of a pulse coherently scattered in the medium. For the collinear geometry and invariable polarisation of the control field considered here, the dielectric susceptibility tensor of the atomic ensemble is diagonal and therefore the polarisation of the probe pulse will not change during its

evolution, remaining circular. Thus, the main characteristic is the pulse intensity. This intensity for the coherent component is determined by the average value of the frequency component of the field-strength operator $\langle E_\mu^+(\mathbf{r}, t) \rangle$. This value in the lowest order of expansion in the probe-radiation intensity can be represented by the graphic expansion

$$\langle E_\mu^+(\mathbf{r}, t) \rangle = \left[\text{thin dashed line} \right] + \left[\text{thick solid line with wavy line} \right] + \left[\text{thick solid line with wavy line} \right] + \dots \quad (1)$$

Here, the wavy and solid lines correspond to the photon and atomic Green functions, respectively. The tops correspond to the interaction of light with atoms of the medium in the dipole approximation. The thin dashed straight lines are the coherent components of the probe input field. The signs at the tops correspond to the choice of a certain type of time ordering of Green functions appearing in the Keldysh technique.

The atomic Green functions $G_m^{(-)}$ for excited states are shown in diagrams (1) by thick solid lines. Unlike thin lines corresponding to free atoms in the ground state, these lines are obtained by the summation of diagrams taking into account spontaneous decay and the interaction of atoms with the classical control field (see below).

The infinite series in the right-hand side of (1) can be summed, by reducing (1) to the Dyson equation

$$\left[\text{thin dashed line} \right] = \left[\text{thin dashed line} \right] + \left[\text{thick solid line with wavy line} \right] \left[\text{thick solid line} \right] \quad (2)$$

Such an approach is convenient for considering the stopping of light in the absence of the counterpropagating control radiation, when the reconstructed probe pulse propagates in the positive direction of the z axis.

When the control field propagates after the repeated switching on in the negative direction of the z axis, it is more convenient to act otherwise. As follows from our analysis (see below), in this case only one of the loops in each diagram in (1) describes the creation of the inverted pulse, while the rest of them take into account the interaction of the probe pulse with atoms during its propagation until a stop and after its reconstruction. Thus, it is convenient to calculate the inverted pulse by grouping diagrams in (1) in the following way:

$$\langle E_\mu^+(\mathbf{r}, t) \rangle_b = \left[\text{thin dashed line} \right] + \left[\text{thick solid line with wavy line} \right] \left[\text{thick solid line} \right] \quad (3)$$

Here, $\langle E_\mu^+(\mathbf{r}, t) \rangle_b$ is the average field strength on a photo-detector taking into account the propagation direction and spectral filtration of the components of control radiation; $\tilde{G}_m^{(-)}$ is the excited-state Green function in which only the terms depending on the mutual orientation of the wave vectors of the control field at the two stages of the system evolution and, therefore, responsible for the formation of the inverted probe pulse, are preserved.

Diagram (3) can be easily interpreted. The thick dashed line satisfying Eqn (2) describes the propagation of the probe pulse in the positive direction of the z axis at the first stage, when the probe field was not switched off yet, the thick wavy line describes the propagation of the pulse in the negative direction after repeated switching on the field. The retarded photon Green function corresponding to this wavy line satisfies the equation similar to (2), but with other initial conditions (see details, for example, in [17]).

To calculate the susceptibility tensor of the atomic ensemble under nonstationary EIT conditions and, hence, to solve the radiation transfer equation of type (2) for photon correlation functions entering (3), it is necessary to determine the explicit form of the atomic Green functions of excited states. This problem also can be solved by using the diagrammatic technique.

In the zero order of expansion in the probe field, the multilevel system shown in Fig. 1b decomposes into a set of two-level subsystems coupled by the control field. Consider one of such subsystems. The index n of the Green function corresponds to one of the Zeeman sublevels of the excited state $|n\rangle \equiv |F', n\rangle$. We denote the lower state of the subsystem under study by $|m'\rangle \equiv |F, m'\rangle$.

The diagrammatic technique gives the graphic equations

$$\left[\text{thick solid line} \right] = \left[\text{thick solid line} \right] + \left[\text{thick solid line with wavy line} \right] + \left[\text{thick solid line with vertical dashed line} \right], \quad (4)$$

$$\left[\text{thick solid line} \right] = \left[\text{thick solid line} \right] + \left[\text{thick solid line with vertical dashed line} \right]$$

for the atomic Green functions in the resonance approximation. Here, the wavy lines correspond to the external control field. The terms containing such lines describe the formation of the high-frequency (optical) coherence of an atom and related variations in the population of different atomic states. The medium is optically transparent for the control field, and therefore this field is assumed specified in the calculation. The thin solid lines correspond to the Green functions of free atoms. The spontaneous decay of the excited state is described by the second term in the first equation of system (4).

System (4) in the analytic form is reduced to two equations

$$\begin{aligned} \frac{dG_m^{(-)}(\mathbf{r}; t, t_0)}{dt} &= -i\delta(t - t_0) - \left(i\frac{E_n}{\hbar} + \frac{\gamma}{2} \right) \\ &\quad \times G_m^{(-)}(\mathbf{r}; t, t_0) + \frac{i}{\hbar} (d_\mu)_{mm'} \mathcal{E}_\mu^{(+)}(\mathbf{r}, t) G_{m'n}^{(-)}(\mathbf{r}; t, t_0), \\ \frac{dG_{m'n}^{(-)}(\mathbf{r}; t, t_0)}{dt} &= -i\frac{E_{m'}}{\hbar} G_{m'n}^{(-)}(\mathbf{r}; t, t_0) \\ &\quad + \frac{i}{\hbar} (d_\mu)_{m'n} \mathcal{E}_\mu^{(-)}(\mathbf{r}, t) G_m^{(-)}(\mathbf{r}; t, t_0). \end{aligned} \quad (5)$$

Here, $E_{m'}$ and E_n are the energies of the ground $|m'\rangle$ and excited $|n\rangle$ states coupled by the control field (see Fig. 1); γ is the spontaneous decay rate of the $|n\rangle$ state; $(d_\mu)_{mm'}$ are the matrix elements of the dipole moment operator of an atom; $\mathcal{E}_\mu^{(+)}(\mathbf{r}, t)$ and $\mathcal{E}_\mu^{(-)}(\mathbf{r}, t)$ are the positive- and negative-frequency components of the control classical field. We

assume that the field amplitude changes instantly at the moment t_1 from \mathcal{E}_0 to zero, and the repeated infinitely rapid switching on occurs at the moment t_2 . The field is assumed monochromatic in the intervals $t < t_1$ and $t_2 < t$. On the one hand, such a formulation of the problem means that the consideration is performed beyond the scope of the usual adiabatic approximation. However, as follows from analysis performed below, probe radiation losses related to transient processes are small in the case under study and can be neglected. On the other hand, the instant change in the parameters of the control field allows us to detect reliably the instant of the probe-pulse stopping and to obtain a number of results analytically.

Note that the control field after switching on can considerably differ from the field that acted at the initial stage. It can have the different frequency, amplitude, propagation direction, etc. To avoid the encumbering of calculations by insignificant details, we will assume that the only parameter that can be changed after repeated switching on is the propagation direction $\mathbf{k}_c \rightarrow \mathbf{k}'_c$. Let us divide the time domain into three intervals: 1) $t < t_1$, 2) $t_1 < t < t_2$, and 3) $t_2 < t$. Let us introduce instead of $G_{m'n}^{(-)}(\mathbf{r}; t, t_0)$ a new unknown function $G_{m'n}^{\prime(-)}(\mathbf{r}; t, t_0)$: $G_{m'n}^{\prime(-)}(\mathbf{r}; t, t_0) = G_{m'n}^{(-)}(\mathbf{r}; t, t_0) \exp(i\omega_c t)$, where ω_c is the control field frequency. By substituting this expression into (5), we obtain in each time interval a system of two equations with constant coefficients. The general solution of this system can be found analytically for arbitrary initial conditions. Solutions in different regions should be sewed at the boundaries of the corresponding time intervals. Taking into account that the Green function has two time arguments t and t_0 and $t \geq t_0$, we obtain six different solutions depending on the intervals (1, 2 or 3) to which times t and t_0 belong. Let us denote different solutions by two additional indices i and j : $G_{ij;mm}^{(-)}(t, t_0)$, where $i, j = 1, 2, 3$ depending on the values of t and t_0 .

We present the two most important solutions as an example. One of them, $G_{11;mm}^{(-)}(\mathbf{r}; t, t_0)$ corresponds to the situation when $t_0 < t_1$ and $t < t_1$. This solution allows us to find the susceptibility tensor at the first stage of the probe-pulse evolution during its propagation in the medium before switching off the control field:

$$G_{11;mm}^{(-)}(\mathbf{r}; t, t_0) = \frac{1}{2} \exp[(-i\Delta_1 - \gamma/2 - \Gamma)(t - t_0)/2] T_1(t - t_0). \quad (6)$$

A similar solution $G_{33;mm}^{(-)}(\mathbf{r}; t, t_0)$ will determine the propagation of the reconstructed pulse at the final stage.

The second important solution $G_{31;mm}^{(-)}(\mathbf{r}; t, t_0)$ corresponds to the situation when $t_0 < t_1$ and $t > t_2$. This solution describes the evolution of the excited state beginning in interval 1 and terminating by emission of a photon to the probe-field mode in interval 3 after repeated switching on the control field. The contribution caused by $G_{31;mm}^{(-)}(t, t_0)$ is responsible for the stopping and 'storage' of light in the medium:

$$G_{31;mm}^{(-)}(\mathbf{r}; t, t_0) = \frac{1}{4} \exp[(-i\Delta_1 - \gamma/2 - \Gamma)(t - t_2 + t_1 - t_0)/2] \times \left\{ \exp[-\gamma(t_2 - t_1)/2] T_1(t_1 - t_0) T_1(t - t_2) - \right.$$

$$\left. - \exp[-i\Delta_1(t_2 - t_1) + i(\mathbf{k}'_c - \mathbf{k}_c)\mathbf{r}] \times \frac{|\Omega|^2}{\Gamma^2} T_2(t_1 - t_0) T_2(t - t_2) \right\}. \quad (7)$$

Here, Δ_1 is the detuning of the control field from the resonance (see Fig. 1b); Ω is the corresponding Rabi frequency; and $\Gamma = [(i\Delta_1 - \gamma/2)^2 - |\Omega|^2]^{1/2}$. Note that because the matrix elements of the atomic dipole moment operators are different, the different $m' \rightleftharpoons n$ transitions have different Rabi frequencies. In the calculations presented below, we will fix the value of Ω for the $m' = \{F = 2, M = -1\} \rightleftharpoons n = \{F' = 1, M' = 0\}$ transition. The excited-state energy in (7) is set equal to zero for simplicity ($E_n = 0$). The auxiliary functions $T_1(\tau)$ and $T_2(\tau)$ are defined by the expressions

$$T_1(\tau) = 1 + \exp(\Gamma\tau) + \frac{(\gamma/2 - i\Delta_1)}{\Gamma} [1 - \exp(\Gamma\tau)],$$

$$T_2(\tau) = 1 - \exp(\Gamma\tau).$$

Unlike the stationary control field, when functions $G_{mm}^{(-)}(\mathbf{r}; t, t_0)$ depend on the difference $t - t_0$ of the time arguments, the Green functions in the case under study depend on each of these arguments. Moreover, the second term in braces in (7) substantially depends on the direction of the wave vectors of the control field at the initial (\mathbf{k}_c) and final (\mathbf{k}'_c) evolution stages. One can easily see that upon the calculation of the polarisation operator in (1) or (2) in the case of $\mathbf{k}'_c = -\mathbf{k}_c$, this term will be nonzero if the initial probe and scattered photons are counterpropagating. This circumstance reflects the fact of momentum preservation upon scattering. In addition, the second term does not decay at the interval $t_1 < t < t_2$, which is explained by the fact that we neglected in calculations the relaxation of the hyperfine atomic coherence of the system in the ground state. The first term decreases in this interval at the rate determined by the spontaneous relaxation of the excited state, and therefore its influence can be neglected for $t_2 - t_1 \gg \gamma^{-1}$.

Other atomic correlation functions can be found similarly. The knowledge of these functions allows one to find the susceptibility tensor of the atomic ensemble in the analytic form. By omitting the details of the calculation and corresponding cumbersome expressions, we consider below the basic results.

3. Results of calculations

Before proceeding to the analysis of lidar probing under EIT conditions, i.e. to the analysis of the formation of the reconstructed inverted pulse, we consider a simpler case of reconstructing the probe pulse without a change in its propagation direction. Such a case is realised if the wave vector of the control field does change its direction during observation ($\mathbf{k}'_c = \mathbf{k}_c$). In this case, the main attention will be devoted to the role of transient processes taking place upon instant switching on and off the control field and considered beyond the scope of the adiabatic approximation, which is commonly used in the EIT theory.

The properties of radiation transmitted forward were analysed by solving numerically Eqn (2). It was found that the parameters of the reconstructed pulse depended most

strongly on the total optical thickness of the medium. Therefore, we will distinguish the cases under study by the optical thickness not modified by EIT effects. The optical thickness of a spherically symmetric atomic cloud of a Gaussian shape for radiation propagating through its centre is $b_0 = (2\pi)^{1/2} \sigma' n_0 r_0$, where σ' is the absorption cross section (in the absence of EIT); n_0 is the concentration of atoms at the cloud centre; r_0 is the dispersion of the corresponding Gaussian distribution (we will call it the cloud radius for brevity).

Different curves in Fig. 2 correspond to different optical thicknesses of clouds for the same instants of switching off the control field $t_1 = 200\gamma^{-1}$ and its subsequent switching on $t_2 = 500\gamma^{-1}$. At small thicknesses, a part of the probe pulse has already propagated through the cloud by the instant t_1 , another part is in the cloud, and a part of the pulse has not entered yet into the cloud. The part of the pulse localised in the cloud produces the long-lived hyperfine coherence of the ground atomic state and will be reconstructed after repeated switching on the control field. The part of probe radiation that had no time to enter the medium by the instant t_1 enters it when the control field is already switched off, propagates through the optically dense medium in which EIT is absent, and is scattered incoherently to other modes. Because the probe-pulse duration was set equal to $50\gamma^{-1}$, this part is

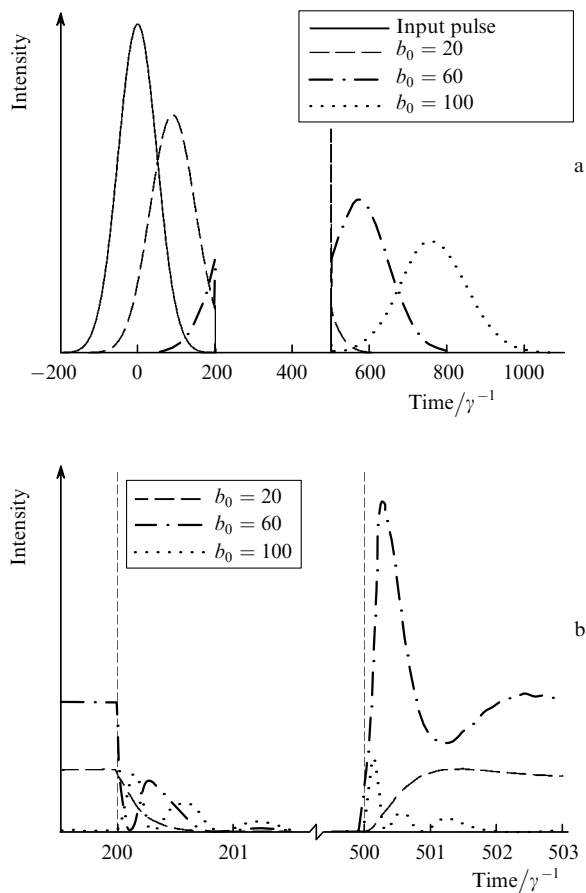


Figure 2. Time dependences of the intensity of the transmitted left-hand circularly polarised probe radiation for different optical thicknesses b_0 of the atomic cloud (a). The control field is switched on at the instant $t_1 = 200\gamma^{-1}$ (light stopping time), the reconstruction of the probe pulse begins at the instant $t_2 = 500\gamma^{-1}$; $\Omega = 0.4\gamma$. Figure 2b shows transient processes at these instants at the extended time scale.

small for $t_1 = 200\gamma^{-1}$. As the cloud thickness increases, the increasing part of the pulse can be retained in the medium.

The instant switching on and off of the control field is accompanied by transient processes, which are illustrated in Fig. 2b. These transient processes lead to the emission of a train of short pulses of total duration γ^{-1} , their number depending on the optical thickness of the medium. This can be explained by the fact that the atomic coherence at the $m' \rightleftharpoons n$ transition is formed upon switching on and decays after switching off the control field for the time of the order of the excited-state lifetime. For this time, the conditions of nonideal EIT are realised in the medium, which are similar to those in the case of a polychromatic control field. A short probe pulse with a relatively broad spectrum is formed. The spectral components of this pulse are absorbed differently during its propagation, a part of them falling into the region of normal dispersion and the other part – into the region of anomalous dispersion. Moreover, a part of components are located outside the atomic resonance region. This leads to a strong distortion of the pulse spectrum during propagation and, hence, to the distortion of the time profile of the pulse. The higher is the optical density of the medium, the stronger are these distortions. The propagation of short pulses with spectral widths comparable with the EIT bandwidth or greater was considered in detail, for example, in [6].

Transient processes proceeding after the instant switching of the control field parameters lead to insignificant losses of the probe-pulse energy, as illustrated in Fig. 3. This figure shows two pulses made coincident on the time axis. The first pulse propagated through the medium in the stationary EIT regime without switching off the control field, while the second pulse was stopped by the method described above. One can see that both these pulses are virtually indistinguishable at the scale used (except a small region related to the transient process, see Fig. 2b). This well agrees with known results [5, 18, 19], according to which rapid switching off the control field leads to small losses if the control field and the group velocity of the probe pulse before switching off were small and the probe-field spectrum was in the transparency region.

Consider now the parameters of the inverted pulse formed after switching on the control field propagating in the negative direction of the z axis. The parameters of this

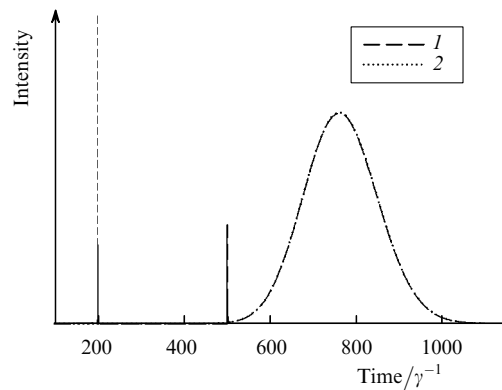


Figure 3. Comparison of the shapes of the reconstructed probe pulse (1) and the pulse propagated through the medium without stopping (2). The optical thickness of the medium is $b_0 = 100$, $t_1 = 200\gamma^{-1}$, $t_2 = 500\gamma^{-1}$, $\Omega = 0.4\gamma$. Pulse (2) is shifted along the time scale by $t_2 - t_1 = 300\gamma^{-1}$ for clearness.

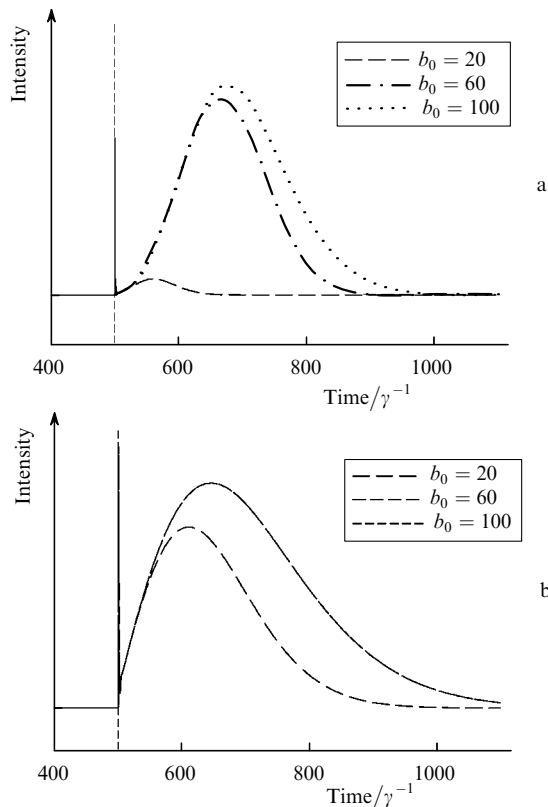


Figure 4. Time dependences of the reconstructed inverted left-hand (a) and right-hand (b) polarised probe pulses for different b_0 , $t_1 = 200\gamma^{-1}$, $t_2 = 500\gamma^{-1}$, and $\Omega = 0.4\gamma$. Probe pulse parameters are as in Fig. 2a.

pulse are found by the direct calculation of diagram (3) by using Eqn (2). Figure 4 shows the shape of inverted pulses recorded at the instant $t_1 = 200\gamma^{-1}$ in clouds of the Gaussian shape of different sizes. The concentration and radius of a cloud are chosen so that the total optical thickness determined by neglecting EIT effects is b_0 . The control field was repeatedly switched on at the instant $t_2 = 500\gamma^{-1}$. It is assumed that the transverse size of the probe beam is considerably smaller than the cloud radius, so that the transverse inhomogeneity of the cloud was neglected. One can see from Fig. 4 that the recording efficiency of the probe Gaussian pulse of a fixed intensity depends on the pulse polarisation and the cloud size. Thus, the left-hand circularly polarised pulse at $b_0 = 20$ is not preserved by the reading instant. The propagation velocity of the right-hand circularly polarised probe pulse for the chosen scheme of operating transitions is substantially lower than that of the left-hand polarised pulse (anisotropy under the EIT conditions are discussed in details in [7]); therefore, the former pulse can be more efficiently used for probing optically thinner media. Note that due to a low velocity of the right-hand polarised pulse, this pulse does not leave the cloud by the instant $t_1 = 200\gamma^{-1}$ for $b_0 = 60$ and more. As a result, in particular, the dependences corresponding to $b_0 = 60$ and 100 in Fig. 4b prove to be indistinguishable.

Figure 5 presents the results of calculation of the inverted pulse stopped at different instants, i.e. recorded in different regions of the Gaussian cloud with the optical thickness $b_0 = 100$. Note that under the EIT conditions, when the pulse velocity in the medium is inversely proportional to the atomic concentration, the instant t_1 of probe-pulse recording determines uniquely the optical path propa-

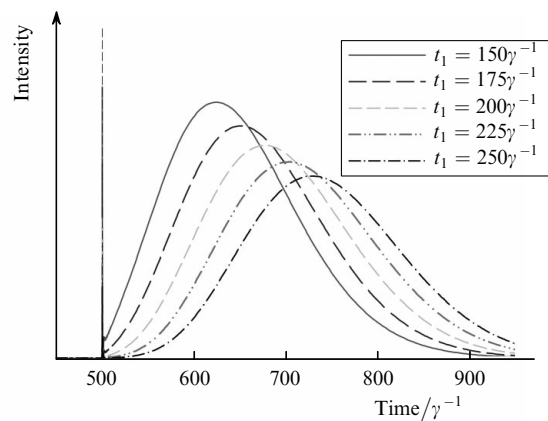


Figure 5. Time dependences of the reconstructed inverted left-hand polarised probe pulse stopped at different instants t_1 for $b_0 = 100$, $t_2 = 500\gamma^{-1}$, $\Omega = 0.4\gamma$. Probe pulse parameters are as in Fig. 2a.

gated by the pulse by this moment. The control field was repeatedly switched on at the same instant $t_2 = 500\gamma^{-1}$ for all the curves. The probe-pulse parameters are as in Fig. 2a. The different shape of these pulses is caused by different penetration depths into the cloud and, thus, demonstrates the possibility of probing clouds in layers.

4. Conclusions

We have studied the propagation of light in the atomic medium under nonstationary EIT conditions. The calculations have been performed beyond the scope of the commonly used adiabatic approximation. Transient processes proceeding after instant switching on and off the control field have been considered. The formation of the inverted reconstructed probe pulse, i.e. the pulse propagating oppositely to its propagation direction before a stop, has been analysed. Based on the analysis performed, the scheme has been proposed for lidar probing atomic or molecular clouds, in which the probe pulse penetrates into the cloud by the specified depth, and information on the state of the latter is obtained from the characteristics of the inverted pulse.

Calculations have been performed for ensembles of ^{87}Rb atoms in the atomic trap. However, the potential possibilities of the method are considerably wider. The method can be used for systems in which the EIT effects and light stopping are possible. In particular, it can be applied for detecting impurity atoms for which (unlike the main component) the condition of EIT appearance is not fulfilled, while the scattering cross section for probe radiation is still sufficiently high. Such impurities can be, for example, clusters of several closely spaced atoms accidentally formed in ultracold clouds. The main advantage of the lidar method over the traditional ‘transmission’ probe method is the possibility to probe object in layers.

Acknowledgements. This work was supported by the Russian Foundation for Basic Research (Grant No. 05-02-16172) and INTAS (Grant No. ID:7904).

References

1. Marangos J.P. *J. Mod. Opt.*, **45**, 471 (1998).
2. Lukin M.D. *Rev. Mod. Phys.*, **75**, 457 (2003).

3. Fleischhauer M., Imamoglu A., Marangos J.P. *Rev. Mod. Phys.*, **77**, 633 (2005).
4. Fleischhauer M. *Europhys. Lett.*, **45**, 659 (1999).
5. Matsko A.B., Novikova I., Scully M.O., Welch G.R. *Phys. Rev. Lett.*, **87**, 133601 (2001).
6. Shakhmuratov R.N., Odeurs J. *Phys. Rev. A*, **71**, 013819 (2005).
7. Datsyuk V.M., Sokolov I.M., Kupriyanov D.V., Havey M.D. *Phys. Rev. A*, **74**, 062610 (2006).
8. Matsko A.B., Rostovtsev Y.V., Kocharovskaya O., Zibrov A.S., Scully M.O. *Phys. Rev. A*, **64**, 043809 (2001).
9. Bajcsy M., Zibrov A.S., Lukin M.D. *Nature*, **426**, 638 (2003);
Andre A., Bajcsy M., Zibrov A.S., Lukin M.D. *Phys. Rev. Lett.*, **94**, 063902 (2005).
10. Moiseev S.A., Ham B.S. *Phys. Rev. A*, **70**, 063809 (2004).
11. Fleischhauer M., Lukin M.D. *Phys. Rev. A*, **65**, 022314 (2002).
12. Kupriyanov D.V., Sokolov I.M., Sukenik C.I., Havey M.D. *Laser Phys. Lett.*, **3**, 223 (2006).
13. Konstantinov O.V., Perel' V.I. *Zh. Eksp. Teor. Fiz.*, **39**, 197 (1960).
14. D'yakonov M.I., Perel' V.I. *Zh. Eksp. Teor. Fiz.*, **47**, 1483 (1964).
15. Keldysh L.V. *Zh. Eksp. Teor. Fiz.*, **47**, 1515 (1964).
16. Lifshitz E.M., Pitaevsky L.P. *Physical Kinetics* (Oxford: Pergamon Press, 1981; Moscow: Nauka, 1979).
17. Datsyuk V.M., Sokolov I.M. *Zh. Eksp. Teor. Fiz.*, **129**, 830 (2006).
18. Liu C., Dutton Z., Behroozi C.H., Hau L.V. *Nature*, **409**, 490 (2001).
19. Dutton Z., Hau L.V. *Phys. Rev. A*, **70**, 053831 (2004).